Hindawi
Advances in Polymer Technology
Volume 2020, Article ID 7879368, 12 pages
https://doi.org/10.1155/2020/7879368

Research Article

Influence of the Preparation Method on Some Characteristics of Alginate/Chitosan/Lovastatin Composites

Duc-Thuan Nghiem,[1] Thuy-Chinh Nguyen,[2,3] Minh-Thanh Do,[2] Thi-Huyen Nguyen,[4] Dai Lam Tran,[2,3] Tran-Dung Hoang,[2] Van-Quan Le,[1] Quoc-Trung Vu,[4] Duy-Trinh Nguyen,[5] and Hoang Thai[2,3]

[1]*Military Hospital 103, Vietnam Military Medical University, 261 Phung Hung, Phuc La, Ha Dong, Hanoi 100000, Vietnam*
[2]*Institute for Tropical Technology, Vietnam Academy of Science and Technology, 18 Hoang Quoc Viet, Cau Giay, Hanoi 100000, Vietnam*
[3]*Graduate University of Science and Technology, Vietnam Academy of Science and Technology, 18 Hoang Quoc Viet, Cau Giay, Hanoi 100000, Vietnam*
[4]*Hanoi National University of Education, No. 136 Xuan Thuy Road, Cau Giay, Hanoi 100000, Vietnam*
[5]*Nguyen Tat Thanh University, 300A Nguyen Tat Thanh, District 4, Ho Chi Minh City 700000, Vietnam*

Correspondence should be addressed to Thuy-Chinh Nguyen; thuychinhhn@gmail.com and Hoang Thai; hoangth@itt.vast.vn

Received 25 October 2019; Revised 30 November 2019; Accepted 12 December 2019; Published 4 January 2020

Guest Editor: Mingqiang Li

This study investigates the effects of direct and indirect dispersion methods for lovastatin solid dispersion (LSD) in alginate (AG)/chitosan (CS) composites on the characteristics and properties of the AG/CS/LSD composites. The preparation method significantly influences the structure, morphology, and LSD size distribution of the composites as well as the drug release of LSD from the samples. The differences in dispersion methods for LSD lead to differences in the interaction between the components, the structure, and the control drug release of LSD. Lovastatin was released from the samples containing LSD in two stages (a fast release stage and a slow release stage), and the drug release content prepared using the indirect method is lower than that prepared using the direct method in the same buffer solution. After 32 h of testing, the released LSD content from the indirect and direct LSD dispersion methods in pH 2 and pH 7.4 buffer solutions was 87–94% and 41–61%, respectively. Drug release kinetics from the above samples in solutions with different pH values was also set up.

1. Introduction

Lovastatin, a natural product with a potential inhibitory effect on HMG-CoA reductase, was synthesized in 1979 and first applied in medicine in 1987. It is absorbed rapidly in the small intestine if administered orally. The plasma concentration of lovastatin reaches its maximum within 4 h. It has a short half-life of 3 h and a low bioavailability of 5% [1]. Lovastatin is widely used to lower cholesterol and reduce the risk of cardiovascular diseases. As lovastatin has poor aqueous solubility, researchers face a great challenge to develop suitable and viable methods and technologies for the preparation of drug samples to enhance the saturation solubility and dissolution velocity of drugs. This shall allow for the achievement of optimum absorption in the systemic circulation as well as bioavailability of drugs in therapy.

Basavaraj et al. used nanotechnology to reduce the particle size of lovastatin from micron size to nanosize level by precipitation process without the use of surfactants or stabilizers [2]. The authors showed methanol and acetone to be suitable solvents for the preparation of lovastatin nanocrystal, at 3 mM concentration of drug. The dissolution rate of nanocrystal drug in methanol and acetone was doubled due to the contact of the drug particles with a larger

surface area of the dissolution medium, and oral bioavailability in biological fluid of nanocrystal drug was increased as compared to the pure lovastatin. Inclusion complex techniques were also used for the preparation of lovastatin systems by kneading method through the combination of excipients (B-cyclodextrin, hydroxypropyl-β-cyclodextrin, randomly methylated B-cyclodextrin, etc.), with lovastatin at different drug-carrier ratios. The solubility of lovastatin in these systems was 2.4 to 3.4 times higher than regular drug formulation [1, 3, 4]. Another technique used for increasing the solubility of lovastatin is the solubilization of surfactant by microemulsion or self-microemulsifying drug delivery system methods. The solubility of the drug in these systems was 1.3 to 2.27 times higher than raw lovastatin [5, 6]. Liquisolid compaction and mesoporous carrier techniques have been studied for the improvement of the solubility of lovastatin [7–10]. These are novel techniques, with complex requirements. The solubility of lovastatin in these systems was increased from 1.8 to 3.42 times.

Solid dispersion is the most popular technique for the preparation of lovastatin systems, with the solubility of lovastatin being 1.2–2.9 times higher than that of pure lovastatin [1]. Solid dispersions in which the drug may be present in the amorphous state offer an attractive means of increasing the solubility and, therefore, potentially increasing the oral bioavailability of these complex compounds. The advantages of the solid dispersion technique are the reduction of particle size of drug crystals, improvement of the drug wettability, and enhancement of the degree of porosity. Amongst the various methods (such as solvent evaporation, melt/cool, coprecipitation, dropping, fusion, physical mixture, kneading, freeze-drying, carrier, grinding, and hot-melt extrusion) and carrier options (for example, modified locust bean gum, sodium starch glycolate, crospovidone, poloxamer F68, polyethyleneglycol, soluplus, acetylsalicylic acid, and mannitol), solid dispersion technique has the potential to prepare lovastatin system for effective therapy [11–14]. In this technique, there are physicochemical interactions between lovastatin and carriers that help to deposit the drug on the surface of carriers.

Owing to the variation of the solid dispersion technique, we chose this technique to investigate the solubility of lovastatin in simulated body fluids. The materials as excipients including chitosan (CS), alginate (AG), crosslinking agent, and gelation agent are used in this study. Chitosan and AG are suitable due to their nontoxic, biocompatible, and biodegradable nature. Moreover, chitosan has a high specific area and high drug loading capacity and can interact with AG by electrostatic binding which occurs between protonated amine group of chitosan and COO^- group of AG [15–22]. AG dissolves well in water and is used in drug preparation as a stabilizer and emulsifier or for coating. The combination of chitosan with AG in the lovastatin solid dispersion could provide a good solubility of lovastatin in water and buffer solutions. Sodium tripolyphosphate (STPP) is a crosslinking agent for chitosan, and calcium chloride ($CaCl_2$) is a gelation agent for AG in the lovastatin solid dispersion. This study focuses on investigating the characterizations and solubility of lovastatin in simulated body fluids in two systems prepared according to two methods: directly combined and indirectly combined dropping methods. The aim is to provide detailed evaluation of the role of excipients and preparation method on the solubility of lovastatin. In the direct dropping method combined with solvent evaporation, we first add lovastatin, STPP, and $CaCl_2$ solution into the AG solution, following which we add this mixture solution into chitosan solution. The solution is then centrifuged to obtain the solid residue which is then freeze-dried to obtain a powder containing solid dispersion lovastatin (D-LSD) with the random dispersion of components. For the indirect dropping method, we first add the lovastatin and $CaCl_2$ solution into the AG solution. Following this, the mixture solution is centrifuged and freeze-dried to obtain the AG/lovastatin powder. Thereafter, the AG/lovastatin powder is covered by chitosan and STPP solution using 3D liquid printer to form chitosan-coated AG/lovastatin solid dispersion (ID-LSD) with bilayer structure on lovastatin.

2. Materials and Methods

2.1. Materials. The following materials and chemicals were purchased from Sigma-Aldrich Co.: AG (AG, viscosity of 300–500 mpa-s), AG (CS, deacetylation >75–85%, PDI = 1.61×10^5 Da), lovastatin (LVS, purity > 98%), and sodium tripolyphosphate (STPP, purity >85%). Some other chemicals are analysis reagents, which were used as received.

2.2. Preparation of Composites of Alginate (AG)/Chitosan (CS)/Lovastatin (LVS) Using Different Methods of LVS Dispersion

2.2.1. Direct Combination Dropping Method. The composites of AG/CS/LSD were prepared using the direct combination dropping method to form D-LSD samples as follows. Firstly, some separated solutions were produced, including 0.05 g of STPP in 10 mL of distilled water (solution S1), 15 mL of $CaCl_2$ 0.002 M (solution S2), 0.02 g of LVS in 10 mL of ethanol (solution S3), 0.1 g of AG in 50 mL of distilled water (solution S4), and 0.1 g of CS in 50 mL of acetic acid 1% (solution S5). Secondly, solutions S1, S2, and S3 were mixed together to obtain a homogenous solution (solution S6). Under ultrasonicating at 20000 rpm, solution S6 was dropped into S4 to form solution S7 and kept in this status for 30 min before dropping into S5 to form solution S8, which was ultrasonicated at 20000 rpm for 60 min before centrifuging to obtain the solid part. The solid part was freeze-dried on a FreeZone 2.5 machine (Labconco, USA) to obtain a composite powder containing solid dispersion lovastatin (D-LSD). The schematic diagram of the preparation procedure of D-LSD samples is shown in Figure 1. The ratio of components and abbreviation of samples is listed in Table 1.

2.2.2. Indirect Combination Dropping Method. The composites of AG/CS/LVS were prepared by the indirect combination dropping method to form ID-LSD samples as follows. Firstly, some individual solutions were produced as follows: 15 mL of $CaCl_2$ 0.002 M (solution S1), 0.02 g of LVS in 10 mL

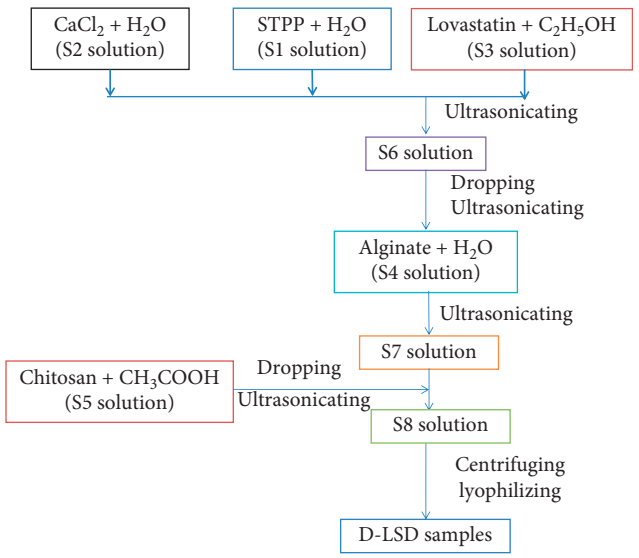

Figure 1: Schematic diagram describing the process of preparing the D-LSD samples.

of ethanol (solution S2), 0.1 g of AG in 50 mL of distilled water (solution S3). Secondly, S2 was dropped into S3 and ultrasonicated for 30 min to obtain a homogenous solution (solution S4). Following this, S4 was heated to 60–70°C and kept at this state for 30 min. At the same time, S1 was dropped into S4 to form AG gelation. This solution was then cooled to room temperature before centrifuging it to obtain the solid part. The solid part was freeze-dried on a FreeZone 2.5 machine (Labconco, USA) to obtain AG/LVS beads in powder.

Following this, 0.01 g of CS and 0.005 g of STPP were dissolved in 4 mL of acetic acid 1% (solution S5), and 0.1 g of the AG/CS beads dispersed into S5 to form solution S6. A total of 2 mL of S6 was pumped into the piston of the 3D liquid printer. Printing process was performed by compiling a g-code script designed for printing to control the nozzle moving in three coordinate axes to cover the surface of the 10×10 cm glass sheet that was heated to 75°C. The print ink (solution S6) was driven out of the printer head to form a 6×6 cm printed area. The printer control was performed by the Repetier-Host software on the computer. The printing process was carried out for 60 min at a speed of 5 mm/s. The width of the printing line was 0.6 mm, and the thickness of the printed layer was 0.2 mm. A total of 2 mL of the remaining S6 was carried out in a manner similar as above. The 3D liquid printer system connected to the computer is presented in Figure 2. The CS-coated AG/LVS beads were obtained in powder and signed as ID-LSD. The schematic diagram for the preparation procedure of ID-LSD samples is presented in Figure 3. The ratio of components and abbreviation of ID-LSD samples having a core-shell structure prepared by print ink solution and 3D liquid printer technique are presented in Table 2.

2.3. Characterization. Infrared (IR) spectra of the samples of AG/CS/LVS composites were recorded by using a Nicolet iS10 (Thermo Scientific, USA) at room temperature in the range of 400–4000 cm^{-1} with the resolution of 8 cm^{-1}. The sample was pressed with KBr to form a pellet before being taken to the IR chamber. Field-emission scanning electron microscope (FESEM) images of samples were taken by using an S-4800 FESEM instrument (Hitachi, Japan). Mean diameter, size distribution, and zeta potential of the samples were determined according to the dynamic light scattering (DLS) method by using a Zetasizer Ver 6.20 particle size analyzer (Malvern Instruments Ltd.). The samples were distributed in distilled water by ultrasonic stirring before being taken to the DLS chamber. *Differential Scanning Calorimetry (DSC) of the samples was measured on a* DSC-131 (SETARAM) in a temperature range from room temperature to 400°C, at a heating speed of 10°C/min in an argon atmosphere. Ultraviolet-visible spectroscopy (UV-Vis, Cintra 40, GBC, USA) was used to determine the drug loading capacity and drug release content from the investigated samples.

2.4. Determination of Drug Loading Capacity. 0.01 g of the sample was dispersed in 200 mL of ethanol, and this solution was stirred continuously for 3 h at 37°C. Then, 10 mL of this solution was withdrawn to record the UV-Vis spectrum. From the absorbance value, drug loading capacity was calculated based on the calibration equation of lovastatin in ethanol ($y = 0.301x + 31269$, with x being the concentration of lovastatin solution and y being absorbance, $\lambda_{max} = 245.547$ nm, linear regression coefficient $R^2 = 0.9931$).

2.5. In Vitro Drug Release Study. The release content of lovastatin from samples was determined by UV-Vis spectroscopy as follows: 0.01 g of samples was added into 200 mL of buffer solutions (simulated gastric fluid (SGF) and simulated intestinal fluid (SIF)), and the solution was stirred at a speed of 400 rpm for 32 hours at 37°C. A sample (5 ml) of the solution was withdrawn from this solution at hourly intervals. The samples were replaced with fresh medium at the same volume. Absorbance values of these solutions were measured by using a UV-Vis spectrophotometer. The percentage drug release was calculated according to the following equation:

$$\%\,\text{lovastatin} = \frac{m_t}{m_o} \cdot 100, \quad (1)$$

where m_t and m_o are the drug contents at t time and initial time, respectively. m_t was determined based on the calibration equations of lovastatin in SGF ($y = 6187x + 0.011$, $\lambda_{max} = 229.97$ nm, $R^2 = 0.996$) and SIF ($y = 3197.2x + 0.0188$; $\lambda_{max} = 239.147$ nm, $R^2 = 0.996$).

2.6. Drug Release Kinetics Study. Drug release kinetics of LVS from the LSD samples evaluated according to the drug release content versus testing time is a popular kinetic model and is as follows:

(i) Zero-order kinetics (ZO): $W_t = W_0 + K_1 \cdot t$ (2)

(ii) First-order kinetics (FO): $\log C = \log C_0 - K_2 \cdot t/2.303$ (3)

Table 1: Ratio of components and abbreviation of D-LSD samples.

No.	STPP weight (g)	$CaCl_2$ 0.002 M volume (mL)	Alginate weight (g)	Chitosan weight (g)	Lovastatin weight (g)	Signed samples
1	0.05	15	0.10	0.10	—	D-LSD1
2	0.05	15	0.10	0.10	0.01	D-LSD2
3	0.05	15	0.10	0.10	0.02	D-LSD3
4	0.05	15	0.10	0.10	0.03	D-LSD4

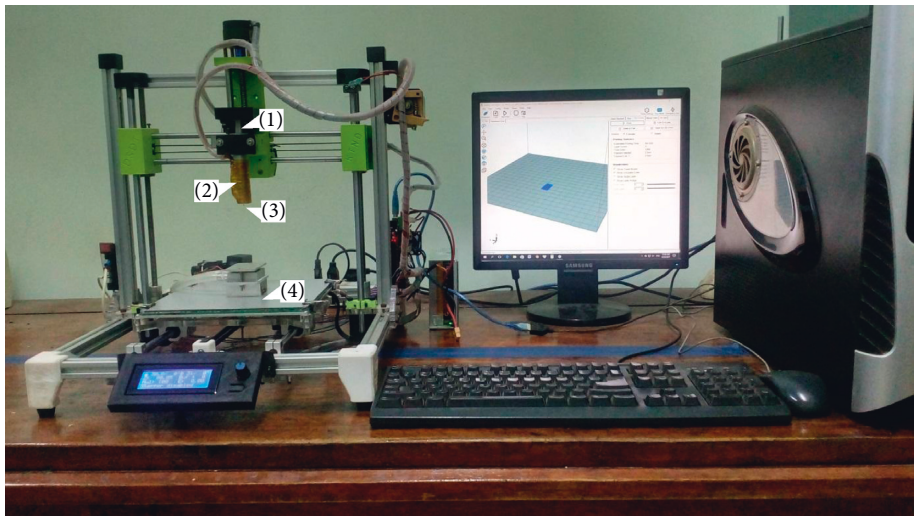

(1) Piston
(2) Cylinder for containing liquid sample
(3) Nozzle
(4) Heated bed

Figure 2: The 3D liquid printer system connected to a computer.

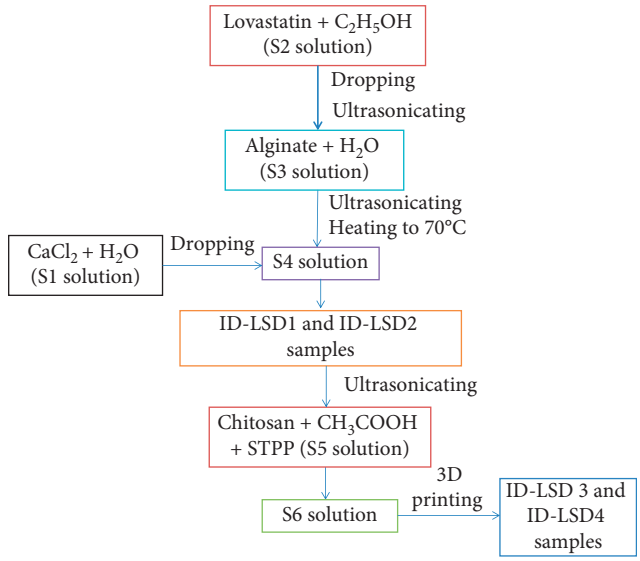

Figure 3: Schematic diagram describing the process of preparing the ID-LSD samples.

Table 2: Ratio of components and abbreviation of ID-LSD samples.

No.	STPP weight (g)	$CaCl_2$ 0.002 M volume (mL)	Alginate weight (g)	Chitosan weight (g)	Lovastatin weight (g)	ID-LSD weight (g)	Signed samples
1	—	15	0.10	—	0.01		ID-LSD1
2	—	15	0.10	—	0.02		ID-LSD2
3	0.05	—	—	0.01	—	0.10 (ID-LSD1)	ID-LSD3
4	0.05	—	—	0.01	—	0.10 (ID-LSD2)	ID-LSD4

(iii) Hixson–Crowell model (HC): $W_0^{1/3} - W_t^{1/3} = K_3 \cdot t$ (4)

(iv) Higuchi model (HG): $W_t = K_4 \cdot t^{1/2}$ (5)

(v) Korsmeyer–Peppas model (KP): $M_t/M_\infty = K_5 \cdot t^n$ (6)

where t is the testing time, K is the drug release constant, n is the diffusion constant, W_t is the weight of drug at the t time, W_0 is the weight of drug at the initial time, M_t/M_∞ is the drug released into the medium, C_0 is the concentration of drug at the initial time, and C is the concentration of drug at the t time.

3. Results and Discussion

3.1. Photo of LSD Samples. Figure 4 presents the photos of LSD samples prepared using direct and indirect dropping methods. The photos clearly indicate that the colors of these samples were not similar. The ID-LSD2 sample was white in color as it consisted of AG and LVS. The D-LSD3 and ID-LSD4 samples were light yellow in color owing to the presence of chitosan.

3.2. Morphology of LSD Samples. The SEM images of LVS, D-LSD, and ID-LSD samples are shown in Figure 5. The LVS has a crystal-bar shape with sizes ranging from 100 to 300 μm [23].

Figure 5 presents the FESEM images of the D-LSD and ID-LSD samples with different LVS contents. It is worth noting that the morphology of LVS had changed in terms of size and shape owing to variations in face dimensions or the appearance/disappearance of some crystal faces [23]. The size of LVS in the D-LSD samples decreased after loading to the AG/CS composites. The LVS was coated by polymers; thus, we did not observe any appearance of LVS bars in the structures of the D-LSD samples. This can be attributed to the formation of hydrogen bonds and electrical interactions between hydroxyl, amine, and carbonyl groups of AG and CS with hydroxyl and carbonyl groups of LVS. In contrast, for the ID-LSD1 and ID-LSD2 samples, the LVS became bar shaped with size ranging from 500 to 3000 nm. The surface of the LVS bars was coated by a thin AG film. As coated by CS (ID-LSD3 and ID-LSD4), the LVS/AG bars were entirely covered by CS layers to form a bilayer structure on the surface of the LVS bars. There was a difference in the morphologies of the D-LSD and ID-LSD samples due to the preparation methods. This variation could cause a modification in the relative crystal degree as discussed later.

3.3. Functional Groups in LSD Samples. The functional groups of LSD samples were indicated in their IR spectra (Figures 6 and 7). In the IR spectra of D-LSD samples (Figure 6), there was a vibration of -CH, -OH, -NH, -C=O, and -C-O groups. The IR spectra of ID-LSD1 and ID-LSD2 were different from the IR spectra of ID-LSD3 and ID-LSD4 because of the CS coating on their surface (Figure 7). The wavenumbers characterized for vibrations of some main functional groups such as -CH, -OH, -NH, -C=O, and -C-O groups in CS, AG, LVS, D-LSD, and ID-LSD samples are listed in Table 3. The shift of position of peaks for -OH, -NH, -C=O, and -C-O groups on the IR of D-LSD and ID-LSD samples as compared with the corresponding peaks on the IR spectrum of AG, CS and LVS confirmed the existence of hydrogen bond and charge interactions between AG, CS, and LVS in investigated samples, as well as the resonance of functional groups. Moreover, the preparation method also affected the functional groups of LSD samples by a slight difference in wavenumbers of functional groups as listed in Table 3.

3.4. Thermal Behavior of LSD Samples. DSC parameters of the D-LSD and ID-LSD samples are listed in Table 4. It can be seen that most LSD samples had the melting temperature that was lower and melting enthalpy that was higher than the equivalent for AG, CS, and LVS. This was caused by the interactions between AG, CS, and LVS. The melting enthalpy of samples was increased remarkably with rising LVS content due to the presence of crystal structure in LVS (D-LSD3 and D-LSD4, ID-LSD1 and ID-LSD2, and ID-LSD3 and ID-LSD4). This phenomenon provides further evidence of the effect of LVS crystal structure on the melting of AG and CS. The melting enthalpy of the ID-LSD samples was higher than that of D-LSD samples. This shows that the preparation method can have an impact on the arrangement of LVS crystal structure in investigated samples [23].

3.5. Size Distribution of LSD Samples. Table 5 and Figure 8 describe the size distribution of LSD samples. The size distribution of D-LSD1 samples ranged from 190.1 nm to 615.1 nm, with the average particle size of 341.3 ± 34.7 nm. As loading LVS, the average particle size of D-LSD2, D-LSD3, and D-LSD4 samples increased but some smaller particles (around 100 nm) were observed at the same time, with the particle intensity percentage of ca. 13%. The increase of particle size followed a general trend for polymer/drug systems because of the appearance of drug-drug and drug-polymer interactions [24].

The preparation method also affected the size distribution of LSD samples. For ID-LSD1 and ID-LSD2, the particle size was 160.7 ± 4.1 nm and 188.8 ± 2.9, respectively. For ID-LSD3 and ID-LSD4, the particle size was 615.1 ± 17.7 nm and 645.7 ± 26.1 nm, respectively. Coating AG/LVS particles by CS was the main reason for the increase in particle size of ID-LSD samples. The transition of zeta potential of ID-LSD3 and ID-LSD4 to a more positive potential as compared to zeta potential of ID-LSD1 and ID-LSD2 also confirmed the coating of CS onto AG/LVS particles due to CS protonated in acidic environment (zeta potentials of ID-LSD1, ID-LSD2, ID-LSD3, and ID-LSD4 are −6.8 mV, −14.8 mV, 5.45 mV, and −9.02 mV, respectively).

3.6. Drug Release of LSD Samples in Different Simulated Body Fluids. Figures 9 and 10 present the drug released content from LVS control, D-LSD, and ID-LSD samples in pH 2 and pH 7.4 solutions. It is clear from the figures that the

(a) (b) (c)

Figure 4: Photos of the LSD samples prepared using different methods: (a) D-LSD3, (b) ID-LSD2, (c) and ID-LSD4.

preparation method had a strong effect on the drug release content from LSD samples. The drug content released from D-LSD samples was much higher than that from the ID-LSD samples at the same testing time. The main reasons for this were the nature of the polymer, combined way of polymers in processing as well as interactions between the drug and polymers. In the D-LSD samples, AG, CS, and LVS were combined, so when D-LSD samples were added into buffer solutions, polymers could swell and dissolve. Hence, LVS placed near the surface of particles would be first diffused into solution, and then, it was the turn of LVS inside of particles. For the ID-LSD samples, LVS was carried by AG before coated with CS; therefore, when taking the ID-LSD samples into buffer solutions, CS layer could limit the diffusion of drug from particles into solutions. As a result, the drug release content from ID-LSD particles was smaller than that from D-LSD samples.

As can be seen from Figures 9 and 10, there was almost no release of LVS from the LVS control in pH 2 solution (only reaching 4.1% after 9 testing hours) and a very fast release in pH 7.4 solution. In contrast, the LVS released from LSD samples in both pH 2 and pH 7.4 solutions and the release of LVS from LSD samples in pH 7.4 solution was much slower than that from the control solution. It was due to the difference in the structure and morphology of LSD sample from LVS control sample. This result confirms that LSD system helped to improve the solubility of LVS in a different pH solution, leading to the enhancement in bioavailability of LVS in treatment.

Again, as can been seen from Figures 9 and 10, LVS released from the LVS control was released in one stage but LVS released from the LSD samples was released in two stages: a fast release stage for the 10 starting hours of the test and a slow release stage in the following hours. After 10 h of testing, the LVS content reached 82.59–92.55% and 41.24–57.19% corresponding to the D-LSD samples and ID-LSD samples, respectively. With increasing LVS content in LSD samples, there is a decreasing trend of the LVS released content. This may be due to the drug-drug interaction leading to the agglomeration of drug in particles when using high drug content, resulting in lowering the diffusion ability of drug from particles into solution.

Figures 9 and 10 also show that pH of the solution had a slight effect on the drug release content from LSD samples. In pH 2 solution, the amine groups in CS were protonated by a proton in the acid environment to form a proton layer around particles leading to the prevention of the release of an LVS part into the solution [16, 25]. Moreover, calcium ion cross-linked with the AG exchanging with ion H^+ leading to the carrier material being converted to water-soluble alginic acid. Sodium ion cross-linked with the chitosan exchanging with ion H^+ but the protonation of amine groups in CS prevailed. Therefore, the drug release content from LSD samples in pH 7.4 solution was higher than that in pH 2 solution.

The LVS content released from ID-LSD3 and ID-LSD4 samples in both investigated pH solutions was generally higher than that from ID-LSD1 and ID-LSD2 samples. For ID-LSD3 and ID-LSD4 samples, the CS content was higher and the drug release was lower. In case of using a higher LVS content (0.03 g of LVS in ID-LSD sample), the drug release content from ID-LSD samples in both pH 2 and pH 7.4 solutions is lower than 20% after 32 h of testing. This is a reason why we do not report about the ID-LSD samples containing 0.03 g of LVS in this article. The drug release from ID-LSD samples was quite complex, and we investigated the reasons behind this phenomenon.

3.7. Drug Release Kinetics of LSD Samples in Different Simulated Body Fluids. Tables 6 and 7 show the LVS release constant and regression coefficient obtained from kinetics equations reflecting LVS released from the samples in pH 2 and pH 7.4 solutions. Zero-order release kinetics describes the process of constant drug release from a drug delivery system when the level of the drug in the blood remains constant throughout the delivery. First-order release kinetics states that change in concentration with respect to change in time is dependent only on concentration. *Hixson–Crowell's* cube root equation is a mathematical *model* used to describe powder dissolution or *drug release* from specific formulations where there is a change in surface area and diameter of particles or tablets. Hence, particles of regular area are proportional to the cube root of its volume. The Higuchi models described the rate of drug release from matrix devices where the drug loading exceeds the solubility in the matrix medium. *Korsmeyer–Peppas model* derived a simple relationship

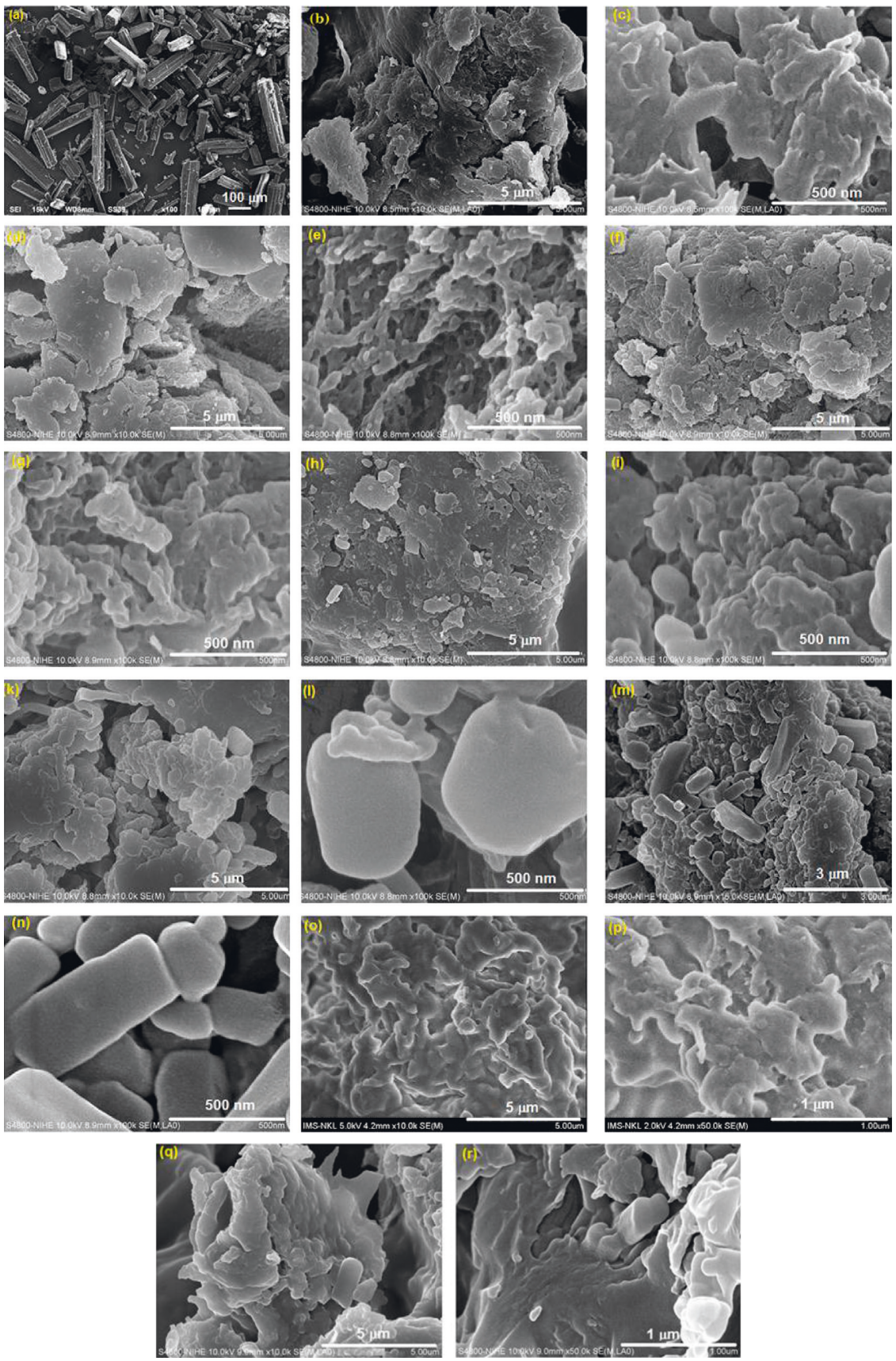

Figure 5: SEM images of (a) lovastatin, (b, c) D-LSD1, (d, e) D-LSD2, (f, g) D-LSD3, (h, i) D-LSD4, (k, l) ID-LSD1, (m, n) ID-LSD2, (o, p) ID-LSD3, and (q, r) ID-LSD4.

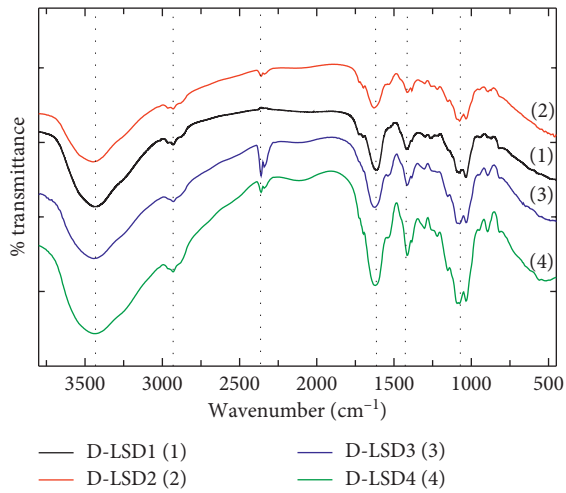

Figure 6: IR spectra of the D-LSD samples.

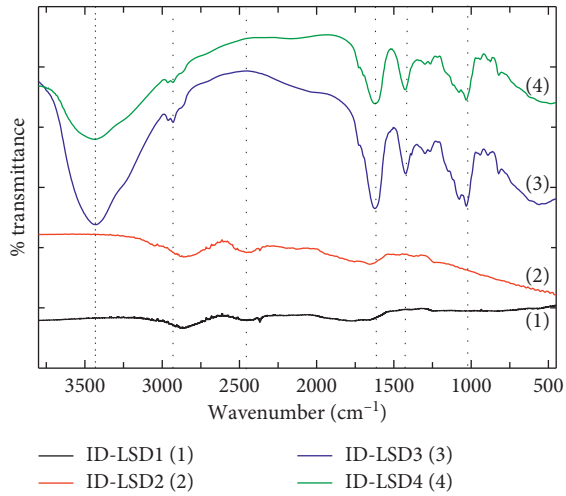

Figure 7: IR spectra of the ID-LSD samples.

Table 3: Vibrations of main functional groups of AG, CS, LVS, D-LSD, and ID-LSD samples.

Sample	Vibration Wavenumbers (cm^{-1})				
	$\nu_{-OH;}\ \nu_{-NH2}$	ν_{-CH}	$\nu_{-C=O}$	δ_{-NH2}	ν_{-C-O}
AG	3448.16	2923.65	1626.64	—	1032.10
CS	3442.46	2924.08	1644.18	1418.87	1027.40
LVS	3540.99	2965.06	1702.02	—	1074.50
D-LSD1	3439.20	2964.77	1613.75	1416.66	1080.70
D-LSD2	3448.76	2930.00	1629.72	1414.02	1075.60
D-LSD3	3444.02	2928.96	1625.30	1414.77	1076.06
D-LSD4	3440.85	2930.04	1629.72	1414.02	1075.60
ID-LSD1	3426.62	2930.06	1622.16	1423.94	1081.54
ID-LSD2	3441.26	2926.46	1621.47	1426.97	1082.90
ID-LSD3	3460.66	2926.28	1630.28	1426.79	1088.00
ID-LSD4	3460.66	2924.26	1619.98	1422.89	1092.69

equation which described which type of dissolution *was followed by a drug release* from a polymeric system. The LVS was released from the samples in two stages: rapid

Table 4: DSC parameters of D-LSD and ID-LSD samples.

Sample	Endothermic peak (°C)	Melting enthalpy (ΔH, J·g^{-1})
AG	119.7	358.6
CS	106.8	48.0
LVS	174.6	90.3
D-LSD3	85.3	236.7
D-LSD4	93.8	405.6
ID-LSD1	106.9	547.0
ID-LSD2	104.9	631.1
ID-LSD3	100.6	497.4
ID-LSD4	98.3	584.1

Table 5: Size distribution of D-LSD and ID-LSD samples.

Sample	Size distribution range (nm)	Main particle size		Average particle size (nm)
		nm	%	
D-LSD1	190.1–615.1	341.3	100	341.3 ± 34.7
D-LSD2	295.3–712.4	449.9	100	449.9 ± 47.3
D-LSD3	58.8–825	99.4	13.8	99.4 ± 10.1
D-LSD4	68.1–825	460.8 118.7 420.5	86.2 13.3 86.7	460.8 ± 68.5 118.7 ± 12.9 420.5 ± 70.9
ID-LSD1	122–190	160.7	100	160.7 ± 4.1
ID-LSD2	142–220	188.8	100	188.8 ± 2.9
ID-LSD3	53–712	615.1	100	615.1 ± 17.7
ID-LSD4	459–825	645.7	100	645.7 ± 26.1

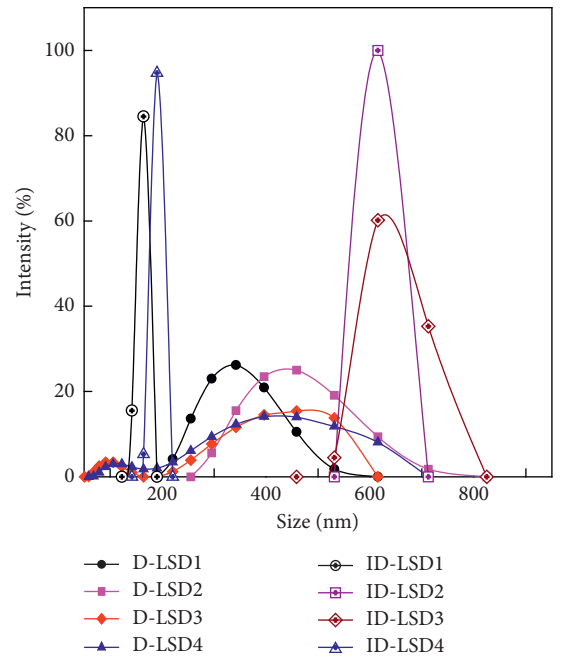

Figure 8: Size distributions of the LSD samples.

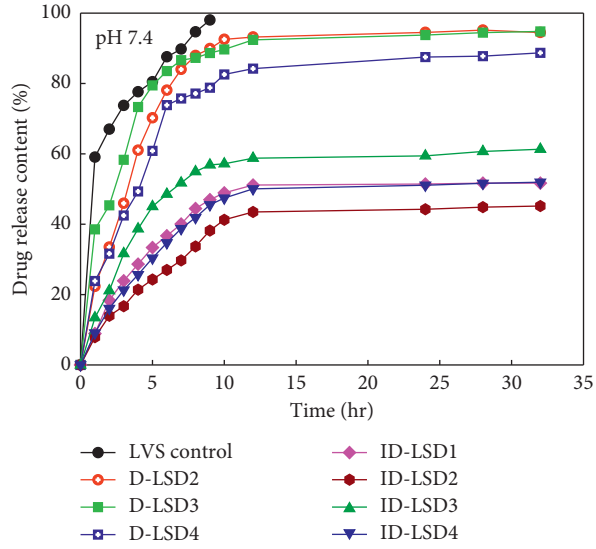

Figure 9: LVS release content from D-LSD and ID-LSD samples in pH 7.4 solution.

Table 6: Release constant (k) and regression coefficient (R^2) obtained from kinetic equations reflecting LVS release from D-LSD and ID-LSD samples in pH 7.4 solution.

Sample		ZO		FO		HG		HC		KP		
		k	R^2	k	R^2	k	R^2	k	R^2	k	n	R^2
D-LSD1	Fast stage	3.10^{-5}	0.9281	−0.1457	0.8359	0.0001	0.9774	-1.10^{-5}	0.9281	0.6521	0.2276	0.9825
	Slow stage	6.10^{-7}	0.9286	−0.0016	0.9315	5.10^{-6}	0.8963	-2.10^{-7}	0.9286	0.0307	0.8620	0.8654
D-LSD2	Fast stage	4.10^{-5}	0.8506	−0.0898	0.7988	0.0002	0.9275	-1.10^{-5}	0.8506	0.4051	0.3820	0.9537
	Slow stage	9.10^{-7}	0.9938	−0.0013	0.9939	8.10^{-6}	0.9888	-3.10^{-7}	0.9938	0.0256	0.8668	0.9785
D-LSD3	Fast stage	7.10^{-5}	0.9278	−0.1336	0.8698	0.0003	0.9659	-2.10^{-5}	0.9278	0.5851	0.2287	0.9821
	Slow stage	2.10^{-6}	0.9740	−0.0026	0.9729	2.10^{-5}	0.9855	-8.10^{-7}	0.9740	0.0517	0.7411	0.9215
ID-LSD1	Fast stage	0.0001	0.8039	−0.2226	0.8487	0.0004	0.8783	-3.10^{-5}	0.8039	0.8007	0.0652	0.9876
	Slow stage	2.10^{-6}	0.9821	−0.0044	0.5808	2.10^{-5}	0.982	-7.10^{-7}	0.9821	0.1477	0.2593	0.8233
ID-LSD2	Fast stage	0.0001	0.9446	−0.1847	0.9016	0.0004	0.987	-4.10^{-5}	0.9446	0.7243	0.1013	0.9963
	Slow stage	1.10^{-6}	0.9551	−0.0053	0.6684	10^{-5}	0.9576	-4.10^{-7}	0.9551	0.1549	0.4023	0.8447
ID-LSD3	Fast stage	7.10^{-5}	0.9865	−0.1751	0.8396	0.0003	0.9894	-2.10^{-5}	0.9700	0.7865	0.1743	0.9916
	Slow stage	2.10^{-6}	0.9618	0.0014	0.8254	2.10^{-5}	0.9548	-6.10^{-7}	0.9618	0.0497	0.8201	0.9460
ID-LSD4	Fast stage	0.0002	0.9283	−0.1805	0.8938	0.0007	0.9830	-5.10^{-5}	0.9283	0.7779	0.0713	0.9994
	Slow stage	4.10^{-6}	0.9929	−0.0033	0.7872	4.10^{-5}	0.9843	-1.10^{-6}	0.9929	0.1160	0.3259	0.9135

ZO: zero-order kinetics; FO: first-order kinetics; HG: Higuchi model; HC: Hixson–Croswell model; KP: Korsmeyer–Peppas model.

release for the first 10 testing hours and slow release in the following hours. In both pH 7.4 and pH 2 solutions, LVS content released from the D-LSD and ID-LSD samples followed Korsmeyer–Peppas model (diffusion/relaxation model) for fast stage ($R^2 > 0.95$) and Hixson–Croswell model for slow stage ($R^2 > 0.92$). It means that in the fast release stage during the first 10 testing hours, the mechanism for LVS release from the D-LSD and ID-LSD samples into solution pH 7.4 was quite complex and combined by processes of polymer swelling, polymer dissolution, and drug diffusion, among others. These results agree with the LVS release process published in some studies [26, 27]. In the slow release stage, LVS content was released from a system having a change on surface area and a diameter of particles according to the erosion mechanism. Comparing regression coefficients obtained from zero-order kinetics and first-order kinetics, the release of LVS from the LSD samples was complied with zero-order kinetics. It confirms that the LVS release rate was constant over a period of testing time [28].

4. Conclusions

In conclusion, we successfully prepared the composites of AG/CS/LVS by using combination dropping methods to form D-LSD samples based on a one-step and two-step procedure, with LVS, AG, CS, $CaCl_2$, and STPP being used as components. For ID-LSD samples, for the first time, we used print ink solution and 3D liquid printer technique to prepare AG/CS/LVS composites having core-shell structure. The difference in combination of components leads to the formation of indirect LSD and direct LSD samples. The ID-

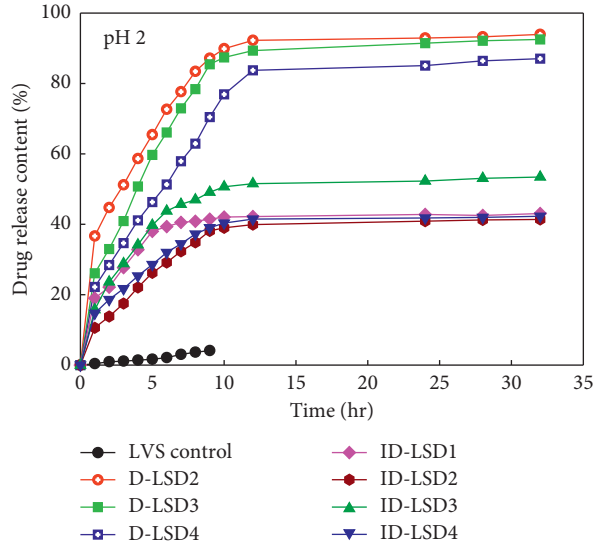

Figure 10: LVS release content from D-LSD and ID-LSD samples in the pH 2 solution.

Table 7: Release constant (k) and regression coefficient (R^2) obtained from kinetic equations reflecting LVS release from D-LSD and ID-LSD samples in pH 2 solution.

Sample		ZO		FO		HG		HC		KP		
		k	R^2	k	R^2	k	R^2	k	R^2	k	n	R^2
D-LSD1	Fast stage	2.10^{-5}	0.9856	−0.0978	0.9483	0.0001	0.9942	-8.10^{-6}	0.9856	0.4118	0.3447	0.9868
	Slow stage	3.10^{-7}	0.9286	−0.0008	0.9301	3.10^{-6}	0.8963	-1.10^{-7}	0.9286	0.0162	0.8855	0.8635
D-LSD2	Fast stage	5.10^{-5}	0.9868	−0.1334	0.9369	0.0002	0.9902	-2.10^{-5}	0.9868	0.5650	0.2384	0.9859
	Slow stage	1.10^{-6}	0.9905	−0.0018	0.9899	1.10^{-5}	0.9970	-4.10^{-7}	0.9905	0.0359	0.8173	0.9967
D-LSD3	Fast stage	6.10^{-5}	0.9986	−0.1313	0.9699	0.0003	0.9759	-2.10^{-5}	0.9986	0.5452	0.2018	0.9799
	Slow stage	2.10^{-6}	0.9506	−0.0019	0.9524	2.10^{-5}	0.9270	-6.10^{-7}	0.9506	0.0374	0.7619	0.9018
ID-LSD1	Fast stage	0.0001	0.9445	−0.1141	0.8909	0.0005	0.9816	-4.10^{-5}	0.9445	0.4716	0.1201	0.9775
	Slow stage	2.10^{-6}	0.9830	−0.0012	0.7870	2.10^{-5}	0.9794	-6.10^{-7}	0.9830	0.0844	0.2725	0.9253
ID-LSD2	Fast stage	0.0001	0.8626	−0.1702	0.9571	0.0006	0.9365	-5.10^{-5}	0.8626	0.6489	0.1213	0.9828
	Slow stage	6.10^{-7}	0.7560	−0.0030	0.8133	5.10^{-6}	0.7999	-2.10^{-7}	0.7560	0.1205	0.4222	0.9422
ID-LSD3	Fast stage	5.10^{-5}	0.9579	−0.1698	0.9181	0.0002	0.9892	-2.10^{-5}	0.9579	0.5584	0.3504	0.9979
	Slow stage	2.10^{-6}	0.8189	0.0063	0.7140	1.10^{-5}	0.8602	-5.10^{-7}	0.8189	0.0977	0.8786	0.8041
ID-LSD4	Fast stage	0.0002	0.9881	−0.1191	0.9566	0.0007	0.9816	-5.10^{-5}	0.9881	0.4619	0.0616	0.9897
	Slow stage	9.10^{-6}	0.8987	−0.0026	0.7216	7.10^{-5}	0.9291	-3.10^{-6}	0.8987	0.0426	0.1644	0.7707

ZO: zero-order kinetics; FO: first-order kinetics; HG: Higuchi model; HC: Hixson–Croswell model; KP: Korsmeyer–Peppas model.

LSD samples had an average particle size in the range of 160.7 ± 4.1–645.7 ± 26.1 nm while the D-LSD samples had a smaller average particle size from 99.38 ± 10.1 nm to 460.8 ± 68.5 nm. The FTIR spectra of LSD samples showed that LVS, CS, and AG interact together, and some peaks at the same position overlapped. The different preparation methods also influenced changes in crystal structure and morphology of LSD samples. The D-LSD samples had more regular morphology than the ID-LSD samples. The LVS released from the D-LSD and ID-LSD samples in pH 2 and pH 7.4 solutions was released in two stages: a rapid release for the first 10 testing hours and a slow release in the following hours. The LVS release content from D-LSD samples was higher than that from the ID-LSD samples. The LVS release content reached 82.59–92.55% and 41.24–57.19% corresponding to the D-LSD samples and ID-LSD samples after 10 testing hours, respectively. The Korsmeyer–Peppas model and Hixson–Croswell model were the most suitable for LVS release in fast stage and slow stage, respectively. The LVS releases process from LSD samples complied with the zero-order kinetics by release rate which was constant over a period of testing time. In general, the one-step method could make D-LSD samples have a more uniform distribution, better interaction of the components, higher drug release content, and better drug release control than ID-LSD samples prepared by the two-step method. These results provide an opportunity to use the D-LSD systems in future applications.

Data Availability

Data are provided in the Supplementary Information files.

Conflicts of Interest

The authors declare no conflicts of interest.

Acknowledgments

This work was supported by the National Foundation for Science and Technology Development in Vietnam (subject code 104.02-2017.17, period of 2017–2020). The authors would like to thank Editage (http://www.editage.com) for English language editing.

References

[1] N. F. Zolkiflee, M. M. R. Meor Mohd Affandi, and A. B. A. Majeed, "Lovastatin: history, physicochemistry, pharmacokinetics and enhanced solubility," *International Journal of Research in Pharmaceutical Sciences*, vol. 8, no. 1, pp. 90–102, 2017.

[2] K. N. Basavaraj, K. D. Ganesh, M. B. Hiren, K. N. Veerendra, and F. V. Manvi, "Design and characterization of nanocrystals of lovastatin for solubility and dissolution enhancement," *Journal of Nanomedicine and Nanotechnology*, vol. 2, no. 2, 2011.

[3] A. Rasheed, C. K. A. Kumar, and V. V. N. S. S. Sravanthi, "Cyclodextrins as drug carrier molecule: a review," *Scientia Pharmaceutica*, vol. 76, no. 4, pp. 567–598, 2008.

[4] A. Mehramizi, E. Asgari Monfared, M. Pourfarzib et al., "Influence of β - cyclodextrin complexation on lovastatin release from osmotic pump tablets (OPT)," *DARU Journal of Pharmaceutical Sciences*, vol. 15, no. 2, pp. 71–78, 2007.

[5] R. P. Patel and M. M. Patel, "Preparation and evaluation of inclusion complex of the lipid lowering drug lovastatin with β-Cyclodextrin," *Dhaka University Journal of Pharmaceutical Sciences*, vol. 6, no. 1, pp. 25–36, 2007.

[6] R. Emőke, B. Tőkés, and S. Emese, "Physical and chemical study of lovastatin inclusion complexes. Bioavailability improvement," *Acta Medica Marisiensis*, vol. 58, no. 5, pp. 326–328, 2012.

[7] V. Viswanath and G. Somasekhar, "Stability enhancement of lovastatin by liquisolid compaction technique," *Journal of Global Trends in Pharmaceutical Sciences*, vol. 5, no. 2, pp. 1933–1939, 2014.

[8] K. Neduri and S. K. Vermula, "Dissolution enhancement of lovastatin by liquisolid compact technique and study of effect of carriers," *International Journal of PharmTech Research*, vol. 6, no. 5, pp. 1624–1632, 2014.

[9] W. Chao, W. Jing, H. Yanchen et al., "Development of a novel starch derived porous silica monolith for enhancing the dissolution rate of poorly water soluble drug," *Materials Science and Engineering: C*, vol. 32, no. 2, pp. 201–206, 2012.

[10] Z. Peng, W. Lihong, S. Changshan et al., "Uniform mesoporous carbon as a carrier for poorly water soluble drug and its cytotoxicity study," *European Journal of Pharmaceutics and Biopharmaceutics*, vol. 80, no. 3, pp. 535–543, 2012.

[11] M. Patel, A. Tekade, S. Gattani, and S. Surana, "Solubility enhancement of lovastatin by modified locust bean gum using solid dispersion techniques," *AAPS PharmSciTech*, vol. 9, no. 4, pp. 1262–1269, 2008.

[12] D. Maji, S. Shaikh, D. Solanki, and K. Gaurav, "Safety of statins," *Indian Journal of Endocrinology and Metabolism*, vol. 17, no. 4, pp. 636–646, 2013.

[13] U. Verma, J. B. Naik, and V. J. Mokale, "Preparation of freeze-dried solid dispersion powder using mannitol to enhance solubility of lovastatin and development of sustained release tablet dosage form," *American Journal of Pharmaceutical Sciences and Nanotechnology*, vol. 1, no. 1, pp. 11–26, 2014.

[14] A. Górniak, M. Gajda, J. Pluta, H. Czapor-Irzabek, and B. Karolewicz, "Thermal, spectroscopic and dissolution studies of lovastatin solid dispersions with acetylsalicylic acid," *Journal of Thermal Analysis and Calorimetry*, vol. 125, no. 2, pp. 777–784, 2016.

[15] K. Agnieszka, M. Aleksandra, M. Justyna, A. Regiel-Futyra, and S. Victor, "Preparation and characterization of alginate/chitosan formulations for ciprofloxacin-controlled delivery," *Journal of Biomaterials Application*, vol. 32, no. 2, pp. 162–174, 2017.

[16] L. Segale, L. Giovannelli, P. Mannina, and F. Pattarino, "Calcium alginate and calcium alginate-chitosan beads containing celecoxib solubilized in a self-emulsifying phase," *Scientifica*, vol. 2016, Article ID 5062706, 8 pages, 2016.

[17] Y. Ji, C. Jie, P. Dan, W. Ying, and W. Zheng, "pH-sensitive interpenetrating network hydrogels based on chitosan derivatives and alginate for oral drug delivery," *Carbohydrate Polymers*, vol. 92, no. 1, pp. 719–725, 2013.

[18] M. Neeraj and K. Gurpreet, "Investigations on polymeric nanoparticles for ocular delivery," *Advances in Polymer Technology*, vol. 2019, Article ID 1316249, 14 pages, 2019.

[19] C. N. Ramesh, K. Rakesh, and J. K. Pandit, "Chitosan coated sodium alginate–chitosan nanoparticles loaded with 5-FU for ocular delivery: in vitro characterization and in vivo study in rabbit eye," *European Journal of Pharmaceutical Sciences*, vol. 47, no. 4, pp. 678–685, 2012.

[20] C. Tingting, L. Shunying, Z. Wenting, L. Zhi, and Z. Qingbing, "Self-assembly pH-sensitive chitosan/alginate coated polyelectrolyte complexes for oral delivery of insulin," *Journal of Microencapsulation*, vol. 36, no. 1, pp. 96–107, 2019.

[21] L. C. Cheng, G. Lu, Y. L. Xin et al., "Development of sustainable carrier in thermosensitive hydrogel based on chitosan/alginate nanoparticles for *in situ* delivery system," *Polymer Composites*, vol. 40, no. 6, pp. 2187–2196, 2019.

[22] P. Mukhopadhyay, S. Maity, S. Mandal, A. S. Chakraborti, A. K. Prajapati, and P. P. Kundu, "Preparation, characterization and in vivo evaluation of pH sensitive, safe quercetin-succinylated chitosan-alginate core-shell-corona nanoparticle for diabetes treatment," *Carbohydrate Polymers*, vol. 182, pp. 42–51, 2018.

[23] R. R. Thenge, S. V. Lonkar, N. M. Mahajan et al., "Modification and characterization of lovastatin crystals," *World Journal of Pharmacy and Pharmaceutical Sciences*, vol. 5, no. 1, pp. 1035–1045, 2015.

[24] C.-Y. Yu, X.-C. Zhang, F.-Z. Zhou, X.-Z. Zhang, S.-X. Cheng, and R.-X. Zhuo, "Sustained release of antineoplastic drugs from chitosan-reinforced alginate microparticle drug delivery systems," *International Journal of Pharmaceutics*, vol. 357, no. 1-2, pp. 15–21, 2008.

[25] T. A. Ahmed and K. M. El-Say, "Development of alginate-reinforced chitosan nanoparticles utilizing W/O nanoemulsification/internal crosslinking technique for transdermal delivery of rabeprazole," *Life Sciences*, vol. 110, no. 1, pp. 35–43, 2014.

[26] L. Ochoa, M. Igartua, R. M. Hernández, A. R. Gascón, M. A. Solinis, and J. L. Pedraz, "Novel extended-release formulation of lovastatin by one-step melt granulation: *In*

vitro and *in vivo* evaluation," *European Journal of Pharmaceutics and Biopharmaceutics*, vol. 77, no. 2, pp. 306–312, 2011.

[27] P. Sandhya, G. Kodali, and A. Fatima, "Formulation and in-vitro characterization of gastro retentive mucoadhesive tablets of Lovastatin," *International Journal of Biological & Pharmaceutical Research*, vol. 5, no. 1, pp. 71–77, 2014.

[28] G. Abhijit, "Achieving zero-order release kinetics using multi-step diffusion-based drug delivery," *Pharmaceutical Technology*, vol. 38, no. 5, pp. 38–42, 2014.